BRACHISTOCHRONES FOR ATTRACTIVE LOGARITHMIC POTENTIAL

Garry J. Tee

Department of Mathematics, University of Auckland

Auckland, New Zealand

Abstract

Brachistochrones are constructed for attractive central force, with logarithmic potential. Each pair of points (except those with the centre between them) are connected by an unique brachistochrone.

AMS subject classification: 70D05, 49J05

1 Logarithmic Potential

Under any force field, the path of quickest descent from one point to another is called the brachistochrone for those points. For any central force, each brachistochrone is in a plane through the startpoint, the endpoint and the centre of force.

Logarithmic potential applies to forces between parallel lines of uniform charge or mass etc. Such problems are inherently 2–dimensional, with every plane normal to the parallel lines having the same potential field. Any force field can be produced on a spaceship (with adequate propellant); but otherwise there do not seem to be any realistic physical instances of 3–dimensional fields with radial symmetry and logarithmic potential. Nonetheless, such 3–dimensional fields can be studied as mathematical problems, with each brachistochrone being a plane curve.

A central logarithmic potential of the form

$$\varphi(r) \;=\; \mu \;\log r \tag{1}$$

where r is the radius from a centre O, gives a force (per unit mass) directed towards O, which is inversely proportional to the radius:

$$F \;=\; \frac{\mu}{r}\;. \tag{2}$$

The unit of time can be scaled so that $\mu = 1$ for attraction, and $\mu = -1$ for repulsion.

For a particle released from rest at A, whose radius is taken as 1, the speed at radius r is $v(r)$ (cf. Tee, 1999, (14)), where

$$\tfrac{1}{2}v(r)^2 \;=\; -\varphi(r) \;=\; -\mu \;\log r, \tag{3}$$

with $r \leq 1$ for attraction and $r \geq 1$ for repulsion. Thus the speed is unbounded as $r \searrow 0$ for attraction, and as $r \nearrow \infty$ for repulsion. Hence,

$$r \;=\; e^{\mu\varphi} \;=\; e^{-\mu v^2/2}, \tag{4}$$

since $\mu = 1/\mu$.

1.1 Radial Motion

For attractive logarithmic potential $\mu = 1$, if the endpoint B lies inside the interval OA then the line AB is the brachistochrone, with the particle falling freely towards the centre, at speed $v(r) = -\mathrm{d}r/\mathrm{d}t$. Hence, the time taken to reach radius $r \leq 1$ is:

$$t \;=\; \int \mathrm{d}t \;=\; \int_r^1 \frac{\mathrm{d}x}{v(x)} \;=\; \int v^{-1}\,\mathrm{d}\left(e^{-v^2/2}\right) \;=\; \int_0^{\sqrt{-2\log r}} e^{-v^2/2}\,\mathrm{d}v. \tag{5}$$

In terms of

$$\mathrm{erf}(z) \;\stackrel{\mathrm{def}}{=}\; \frac{2}{\sqrt{\pi}}\int_0^z e^{-u^2}\mathrm{d}u, \tag{6}$$

this can be written as

$$t(r) \;=\; \sqrt{\pi/2}\,\mathrm{erf}(\sqrt{-\log r}). \tag{7}$$

Hence as $r \searrow 0$, the time for falling from radius 1 to r approaches the limit:

$$t(0) \;=\; \sqrt{\pi/2}\,\mathrm{erf}(\infty) \;=\; \sqrt{\pi/2} \;=\; 1{\cdot}2533141373155003\ . \tag{8}$$

This limit can conveniently be abbreviated, by saying that the particle falls to the centre at time $t(0)$.

Figure 1 shews a graph of radius versus time, for a particle falling to the centre.

For repulsive logarithmic potential ($\mu = -1$), if the starting point A is inside the interval OB then the line AB is the brachistochrone, with the particle moving freely outwards in the radial direction, with speed $v(r) \;=\; \mathrm{d}r/\mathrm{d}t$. Hence, the time to reach radius $r > 1$ is:

$$t \;=\; \int \mathrm{d}t \;=\; \int_1^r \frac{\mathrm{d}x}{v(x)} \;=\; \int v^{-1}\,\mathrm{d}\left(e^{v^2/2}\right) \;=\; \int_0^{\sqrt{2\log r}} e^{v^2/2}\,\mathrm{d}v. \tag{9}$$

Figure 2 shews a graph of radius versus time, for a particle repelled radially from the centre. For each r, t is evaluated by numerical integration of the integral in (9).

2 Formulæ for Brachistochrones

Brachistochrones for central forces have been constructed (Tee, 1999) as the orbits of associated free particles under transformed central forces. The family of brachistochrones starting at a fixed point A (whose polar coordinates are taken as $r = 1,\ \vartheta = 0$) can be parametrized by the angular momentum K of the associated free particle. Here, it is more convenient to parametrize them by $J = 2K^2$.

Figure 1: Radius versus Time, Radial Motion for Attractive Logarithmic Potential

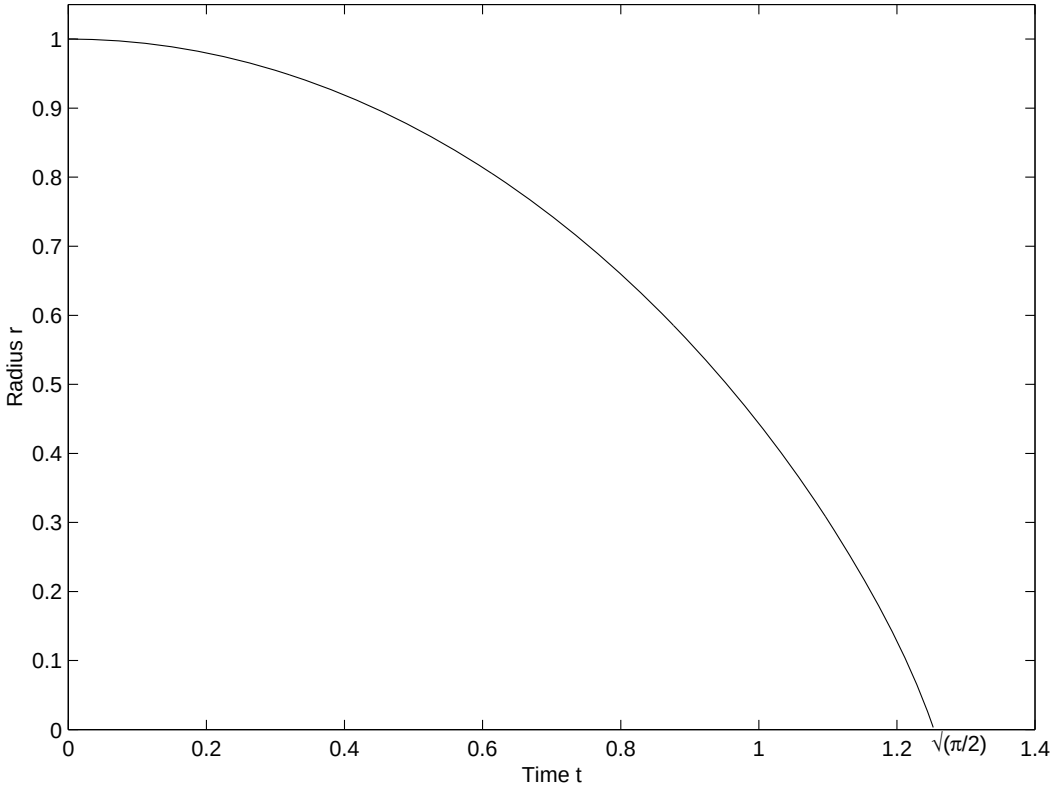

Figure 2: Radius versus Time, Radial Motion for Repulsive Logarithmic Potential

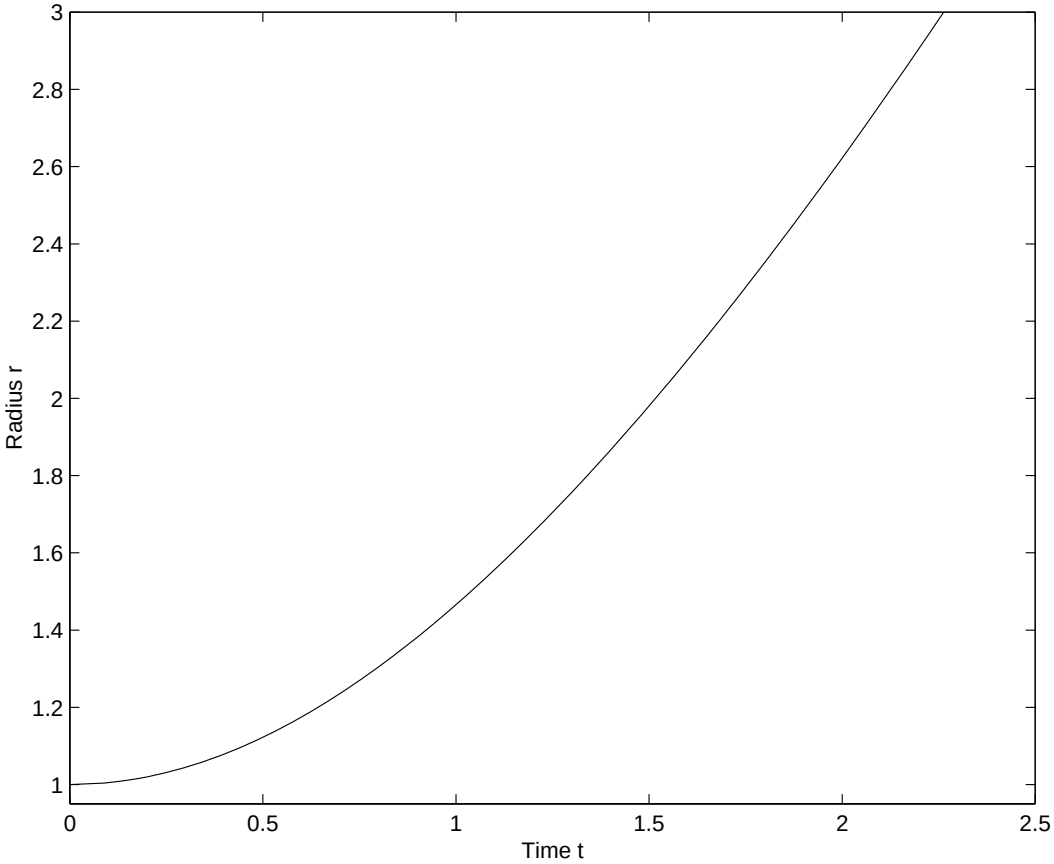

Hereafter, we consider only $J > 0$, since radial motion has been dealt with in §1.1.

Equations (23), (31) and (37) in (Tee, 1999) then give angle ϑ, arclength s and time t, each as a definite integral between radius 1 and r:

$$\vartheta \;=\; \int_1^r \frac{\mathrm{d}x}{\pm x\sqrt{\frac{2x^2}{Jv(x)^2}-1}} \;=\; \int_0^{\mu\log r} \pm\mu\,\sqrt{\frac{-J\psi}{e^{2\mu\psi}+J\psi}}\;\mathrm{d}\psi\;, \tag{10}$$

$$s \;=\; \int_1^r \frac{\mathrm{d}x}{\pm\sqrt{1-\frac{Jv(x)^2}{2x^2}}} \;=\; \int_0^{\mu\log r} \frac{\mu e^{2\mu\psi}\;\mathrm{d}\psi}{\pm\sqrt{e^{2\mu\psi}+J\psi}}\;, \tag{11}$$

$$t \;=\; \int_1^r \frac{\mathrm{d}x}{\pm\sqrt{v(x)^2\left(1-\frac{Jv(x)^2}{2x^2}\right)}} \;=\; \int_0^{\mu\log r} \frac{\mu e^{2\mu\psi}\;\mathrm{d}\psi}{\pm\sqrt{2\psi\,(e^{2\mu\psi}+J\psi)}}\;. \tag{12}$$

Here, $\psi = \varphi(x)$, with the particle released from rest at A always having $\psi \le 0$. In each of these integrals the positive square root is to be taken where radius increases with t, and the negative square root is to be taken where radius decreases with t.

2.1 Equation for Apsidal Radius R

The orbit of the associated free particle with angular momentum K has an apsidal radius R, if and only if $K = R/v(R)$ (cf. Tee, 1999, (25)). In terms of $J = 2K^2$,

$$J \;=\; \frac{2R^2}{v(R)^2} \;=\; \frac{R^2}{-\mu\,\log\,R}, \tag{13}$$

in view of (3).

At any apse,

$$0 \;=\; \frac{\mathrm{d}r}{\mathrm{d}\vartheta} \;=\; \frac{\mathrm{d}\varphi}{\mathrm{d}\vartheta} \;=\; \frac{\mathrm{d}r}{\mathrm{d}s} \;=\; \frac{\mathrm{d}\varphi}{\mathrm{d}s} \;=\; \frac{\mathrm{d}r}{\mathrm{d}t} \;=\; \frac{\mathrm{d}\varphi}{\mathrm{d}t}\;. \tag{14}$$

The integrands in (10), (11) and (12) are the reciprocals of these derivatives. Therefore, each of those 6 integrands has an integrable singularity at the apse $x = R,\ \psi = \mu\,\log\,R$.

The *total angle* of a particle on a brachistochrone is defined as $\int \mathrm{d}\vartheta$. If the particle has wound more than once around the centre, then the total angle is greater than 2π.

3 Attractive Logarithmic Potential

For attractive force, $\mu = 1$. For fixed $J > 0$, equation (13) gives an equation in R:

$$R^2 \;=\; -J\,\log\,R. \tag{15}$$

As R decreases from 1 towards 0, R^2 decreases monotonically towards 0, whilst $-J\,\log\,R$ increases monotonically and unboundedly from 0; so that the equation (13) has exactly one real root $R \in (0,1)$. Therefore, each brachistochrone has one apse, with r decreasing from 1 to the apsidal radius $R > 0$ on the first half–arch, and increasing from R to 1 on the second half–arch.

Hence, the brachistochrones can conveniently be parametrized by the minimum radius R, rather than by J.

With $\mu = 1$, (13) shews that, as R increases between 0 and 1, J increases monotonically, with $J \searrow 0$ as $R \searrow 0$, and $J \nearrow \infty$ as $R \nearrow 1$.

3.1 Equations For Brachistochrone

Taking the negative square roots in (10) (11) (12), we get integral expressions for angle, arclength and time as functions of radius on the first half-arch; each with the minimum radius R as a parameter:

$$\Theta(r,R) = \int_{\log r}^{0} \sqrt{\frac{R^2\psi}{\log R\, e^{2\psi} - R^2\psi}}\, \mathrm{d}\psi \ , \tag{16}$$

$$S(r,R) = \int_{\log r}^{0} \frac{e^{2\psi}}{\sqrt{e^{2\psi} - \frac{R^2}{\log R}\psi}}\, \mathrm{d}\psi \ , \tag{17}$$

$$T(r,R) = \int_{\log r}^{0} \frac{e^{2\psi}}{\sqrt{2\psi\left(\frac{R^2}{\log R}\psi - e^{2\psi}\right)}}\, \mathrm{d}\psi \ . \tag{18}$$

Each brachistochrone is symmetric about each apsidal line; and hence on the second half–arch the positive square roots are taken in (10), (11) and (12), giving

$$\vartheta = 2\Theta(R,R) - \Theta(r,R),\ s = 2S(R,R) - S(r,R),\ t = 2T(R,R) - T(r,R). \tag{19}$$

Or, if angle ω, arclength σ and time τ are measured from the apse, then the complete brachistochrone is given in terms of r by the integrals

$$\omega = \pm \int_{\log R}^{\log r} \sqrt{\frac{R^2\psi}{\log R\, e^{2\psi} - R^2\psi}}\, \mathrm{d}\psi \ , \tag{20}$$

$$\sigma = \pm \int_{\log R}^{\log r} \frac{e^{2\psi}}{\sqrt{e^{2\psi} - \frac{R^2}{\log R}\psi}}\, \mathrm{d}\psi \ , \tag{21}$$

$$\tau = \pm \int_{\log R}^{\log r} \frac{e^{2\psi}}{\sqrt{2\psi\left(\frac{R^2}{\log R}\psi - e^{2\psi}\right)}}\, \mathrm{d}\psi \ . \tag{22}$$

3.1.1 Computation of Brachistochrones

The integral (16) for ϑ has a singularity in the derivative of the integrand at $\psi = 0$, and when $r = R$ it has an integrable singularity at $\psi = \log R$. Those singularities may be eliminated by an appropriate change of variable, to produce a smooth integrand which is suitable for quadrature by Romberg integration.

In (16), substitute

$$\log r = \psi(\kappa) = \tfrac{1}{2} \log R\, (1 - \cos\kappa) = \log R\, \sin^2(\kappa/2), \tag{23}$$

so that as ψ decreases from 0 to $\log R$, κ increases from 0 to π, and

$$\kappa = \kappa(\psi) = \arccos\left(1 - \frac{2\psi}{\log R}\right) \ . \tag{24}$$

Now,

$$\cos^2(\kappa/2) \;=\; 1 - \sin^2(\kappa/2) \;=\; 1 - \frac{\log\, r}{\log\, R} \;=\; \frac{\psi - \log\, R}{-\log\, R}, \tag{25}$$

and therefore

$$\begin{aligned} \mathrm{d}\psi \;&= \log\, R\, \sin(\kappa/2)\, \cos(\kappa/2)\, \mathrm{d}\kappa \\ &= \;-\; \sin(\kappa/2)\, \sqrt{-\log\, R\, (\psi - \log\, R)}\, \mathrm{d}\kappa. \end{aligned} \tag{26}$$

Then the integral (16) becomes

$$\Theta(r, R) \;=\; -R\, \log\, R \int_0^{\kappa(\log\, r)} \sin^2(\kappa/2)\, \sqrt{\frac{\psi - \log\, R}{R^2\psi - \log\, R\, e^{2\psi}}}\, \mathrm{d}\kappa, \tag{27}$$

where the function $\kappa(\psi)$ is given by (24) and the inverse function $\psi(\kappa)$ is given by (24).

In (27) the integrand is smooth for all $r \in (R, 1]$. But, as $r \searrow R$, $\psi \searrow \log\, R$, and hence the argument of the square root approaches the form $0/0$.

In order to avoid that indeterminate expression, substitute

$$w(\kappa) \;=\; \psi - \log\, R \;=\; -\log\, R\, \cos^2(\kappa/2), \tag{28}$$

so that

$$x \;=\; e^{\psi} \;=\; e^{w + \log\, R} \;=\; Re^{w}. \tag{29}$$

Then, (27) becomes

$$\Theta(r, R) \;=\; \int_0^{\kappa(\log\, r)} \frac{-\log\, R\, \sin^2(\kappa/2)}{\sqrt{1 - \log\, R\, \mathcal{F}(-\log\, R\, \cos^2(\kappa/2))}}\, \mathrm{d}\kappa\ , \tag{30}$$

where

$$\mathcal{F}(w) \;\stackrel{\mathrm{def}}{=}\; \frac{e^{2w} - 1}{w} \qquad (w \neq 0), \tag{31}$$

and $\mathcal{F}(0) \stackrel{\mathrm{def}}{=} 2$ (for continuity).

For $|w| \geq \delta$ for some suitable $\delta < 1$ (e.g. $\delta = 10^{-3}$), $\mathcal{F}(w)$ can safely be evaluated directly from (31). But for $|w| < \delta$, $\mathcal{F}(w)$ should be evaluated from the rapidly convergent power series:

$$\mathcal{F}(w) \;=\; \frac{2}{1!} + \frac{2(2w)}{2!} + \frac{2(2w)^2}{3!} + \frac{2(2w)^3}{4!} + \ldots\ . \tag{32}$$

In this manner, the integral expression (30) for $\Theta(r, R)$ can be computed by Romberg integration with respect to κ. In particular, the apsidal angle

$$\Theta(R, R) \;=\; \int_0^{\pi} \frac{-\log\, R\, \sin^2(\kappa/2)}{\sqrt{1 - \log\, R\, \mathcal{F}(-\log\, R\, \cos^2(\kappa/2))}}\, \mathrm{d}\kappa\ , \tag{33}$$

can be computed by Romberg integration with respect to κ.

3.1.2 Bound for Apsidal Angle

For attractive central force proportional to $1/r^n$, with real $n > 1$, Ron Keam has proved that (Tee, 1999, footnote to (74)) as $R \searrow 0$, the limit for the apsidal angle is $\pi/(n+1)$, and hence the total angle has limit $2\pi/(n+1)$. Here we consider logarithmic potential with $n = 1$. The limit $\frac{1}{2}\pi$ of Keam's angle as $n \searrow 1$ suggests that the apsidal angle has the limit $\frac{1}{2}\pi$ as $R \searrow 0$, and hence the total angle has the limit π. (The angle π cannot be attained, since the particle cannot pass through the singularity at the centre, in any physically meaningful problem).

Substituting (3) (with $\mu = 1$) into (Tee, 1999, (27)), we get the expression for ϑ in the form:

$$\vartheta \;=\; \Theta(r,R) \;=\; \int_r^1 \frac{\mathrm{d}x}{x\,\sqrt{\frac{\log R}{\log x}\cdot\frac{x^2}{R^2} - 1}}\;. \tag{34}$$

Substituting

$$x \;=\; \frac{R}{z}\;, \tag{35}$$

so that z increases from R to 1 as x decreases from 1 to R, and

$$\mathrm{d}x \;=\; \frac{-R}{z^2}\,\mathrm{d}z, \tag{36}$$

equation (34) becomes

$$\begin{aligned}\Theta(r,R) \;&=\; \int_R^{R/r} \frac{\mathrm{d}z}{z\,\sqrt{\frac{\log R}{z^2(\log R - \log z)} - 1}} \\ &=\; \int_R^{R/r} \frac{\mathrm{d}z}{\sqrt{\frac{\log R}{\log R - \log z} - z^2}} \;=\; \int_R^{R/r} \frac{\mathrm{d}z}{\sqrt{\frac{\log z}{\log R - \log z} + 1 - z^2}}\;.\end{aligned} \tag{37}$$

Substituting

$$z \;=\; \sin\alpha, \tag{38}$$

this reduces to

$$\Theta(r,R) \;=\; \int_{\arcsin(R)}^{\arcsin(R/r)} \frac{\mathrm{d}\alpha}{\sqrt{1 + \frac{\sec^2\alpha\;\log\sin\alpha}{\log(R/\sin\alpha)}}}\;. \tag{39}$$

(This integrand is indeterminate at each bound, and its derivative has a singularity at the lower bound. Hence, ϑ should be computed by (30).)

In particular, the apsidal angle is

$$\Theta(r,R) \;=\; \int_{\arcsin(R/r)}^{\pi/2} \frac{\mathrm{d}\alpha}{\sqrt{1 + \frac{\sec^2\alpha\;\log\sin\alpha}{\log(R/\sin\alpha)}}} \;=\; \int_0^{\pi/2} \Xi(\alpha)\;\mathrm{d}\alpha, \tag{40}$$

where

$$\Xi(\alpha) \;\stackrel{\text{def}}{=}\; \frac{1}{\sqrt{1 + \frac{\sec^2\alpha\;\log\sin\alpha}{\log(R/\sin\alpha)}}} \qquad (\alpha > \arcsin R), \tag{41}$$

and

$$\Xi(\alpha) \;\stackrel{\text{def}}{=}\; 0 \qquad (\alpha \le \arcsin R). \tag{42}$$

Thus, for each $\alpha \in (0,\pi)$, $\Xi(\alpha)$ is a continuous function of R; which is the constant 0 for $R > \sin\alpha$, and it is the integrand in (39) for $R \le \sin\alpha$. As $R \searrow$

$0,\ \log(R/\sin\alpha) \searrow -\infty$; and hence $\Xi(\alpha) \nearrow 1$, for all $\alpha \in (0, \pi)$. (The convergence of $\Xi(\alpha)$ to 1 is not uniform in α).

Therefore, as $R \searrow 0$, the apsidal angle $\Theta(R, R)$ converges to $\frac{1}{2}\pi$, and the total angle of the complete brachistochrone converges to π.

Table 1 gives the apsidal angle for $R = 10^{-m},\ m = 1, 2, \ldots, 8$. Even with $R = 10^{-8}$ (which requires rather delicate computation by (33)), the apsidal angle 1·52763786999141 differs from the limit $\frac{1}{2}\pi = 1{\cdot}57079632679489661$ by 0·043 .

Table 1

m	R	x	**Apsidal Angle**	**Extrapolation**
1	10^{-1}	1/1	1·18454904348185	1·57065542051970
2	10^{-2}	1/2	1·38567877967839	1·57063431294604
3	10^{-3}	1/3	1·45182977320007	1·57065075063140
4	10^{-4}	1/4	1·48298052830808	1·57078376162025
5	10^{-5}	1/5	1·50108588140844	1·57088727006925
6	10^{-6}	1/6	1·51296377451786	1·57061423215590
7	10^{-7}	1/7	1·52137031732430	1·57151073866118
8	10^{-8}	1/8	1·52763786999141	1·52763786999141

The sequence of 8 apsidal angles given in Table 1 can be extrapolated in various ways, to estimate their limit as $R \searrow 0$. However, their convergence is slower than linear, so that even Aitken acceleration (applied iteratively) does not provide much improvement. Simple polynomial interpolation (by polynomials in R) to $R = 0$ cannot be expected to work well here, since most of the tabular points are very close to $R = 10^{-8}$.

However, if we take $x = -1/\log_{10} R$ as the independent variable, then the tabulated values are given for $x = \frac{1}{1}, \frac{1}{2}, \cdots, \frac{1}{7}, \frac{1}{8}$. Hence, if we construct the interpolation polynomials in x for suitable subsets of these 8 points, then we expect their values at $x = 0$ to give improved estimates of the limit $\frac{1}{2}\pi$.

In the column **Extrapolation** in Table 1, row m gives the result of polynomial extrapolation from $x = 1/8, 1/7, \cdots, 1/m$ to $x = 0$. Even linear extrapolation (from $x = 1/8, 1/7$) reduces the error from 0·043 to 0·00072, and quartic extrapolation (from $x = 1/8, 1/7, 1/6, 1/5, 1/4$) reduces the error to 0·000013 .

We have shewn that the total angle has the upper bound π. Therefore, no brachistochrone connects points A and B, if the interval AB passes through the centre O. With such an endpoint B the particle could fall down the radius vector OA until it gets very close to the centre 0, then smoothly swerve close to the centre around to the radius vector OB and rise up it to B at radius $\rho \leq 1$. For such a smooth path from A to B the passage time has (cf. (7)) the least upper bound

$$\eta(\rho) \ \stackrel{\text{def}}{=}\ t(0) + (t(0) - t(\rho)) \ = \ \sqrt{\pi/2}(2 - \operatorname{erf}(\sqrt{-\log\,\rho})). \tag{43}$$

3.1.3 Pictures of Brachistochrones, for Attractive Inverse Square Force

Figure 3 shews the complete brachistochrones from A for minimum radius $R = 0{\cdot}005\ (0{\cdot}005)\ 0{\cdot}05\ (0{\cdot}05)\ 0{\cdot}95$, with ϑ computed for many values of r by Romberg integration of (30). The dashed curve is the apsidal locus, which separates the first half–arches from the second half–arches.

Figure 3: Brachistochrones, for minimum radius R = 0.005 (0.005) 0.05 (0.05) 0.95

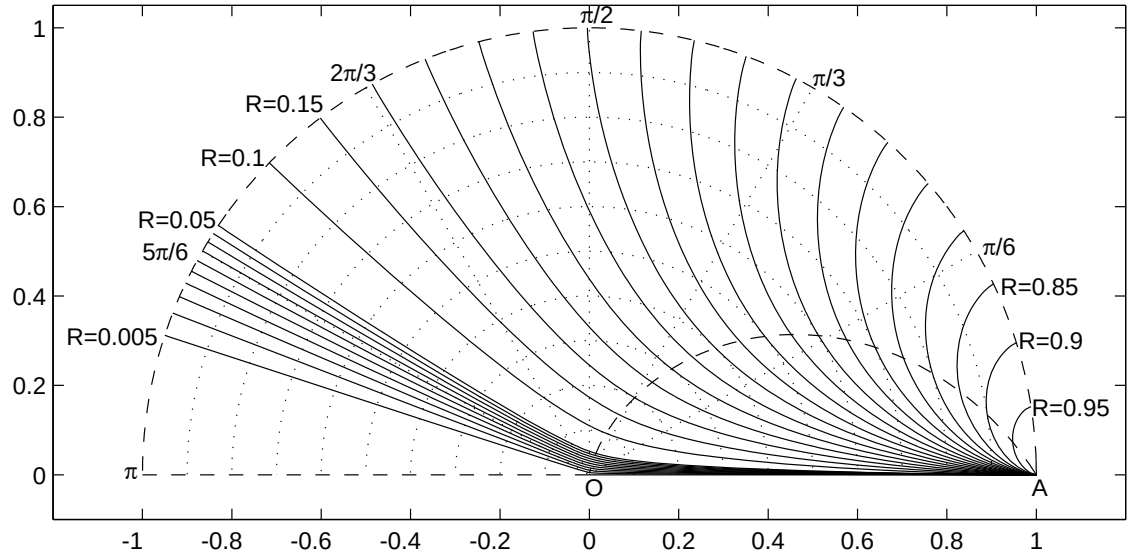

Note that the small complete brachistochrones do indeed resemble complete cycloid arches, as expected. As $R \searrow 0$, the first half–arch converges towards the initial radius vector OA, and the second half–arch converges towards the radius vector at the total angle.

Figure 3 displays the very slow convergence of the total angle to π, as $R \searrow 0$.

3.2 Arclength as a Function of Radius

The integral (17) for s has an integrable singularity at $\psi = \log R$, when $r = R$. Apply the substitution

$$u \;=\; \sqrt{\psi - \log\, R}, \tag{44}$$

so that

$$u^2 \;=\; \psi - \log\, R \tag{45}$$

and

$$e^{\psi} \;=\; Re^{u^2}. \tag{46}$$

Then the equation for S becomes:

$$S(r,R) \;=\; \int_{\sqrt{\log(r/R)}}^{\sqrt{\log(1/R)}} \frac{2Re^{2u^2}}{\sqrt{\mathcal{F}(u^2) - \frac{1}{\log\, R}}}\ \mathrm{d}u\ , \tag{47}$$

where the function $\mathcal{F}$ is to be evaluated as with (31).

In particular, the arclength to the apse is

$$S(R,R) \;=\; \int_{0}^{\sqrt{\log(1/R)}} \frac{2Re^{2u^2}}{\sqrt{\mathcal{F}(u^2) - \frac{1}{\log\, R}}}\ \mathrm{d}u\ . \tag{48}$$

And these transformed integrals are suitable for Romberg integration with respect to u.

3.2.1 Graphs of Radius versus Arclength

Figure 4 shews graphs of r versus s for various values of the minimum radius R, with s computed for various values of r by Romberg integration of (47). Each graph is symmetric about the line $s = S(R, R)$.

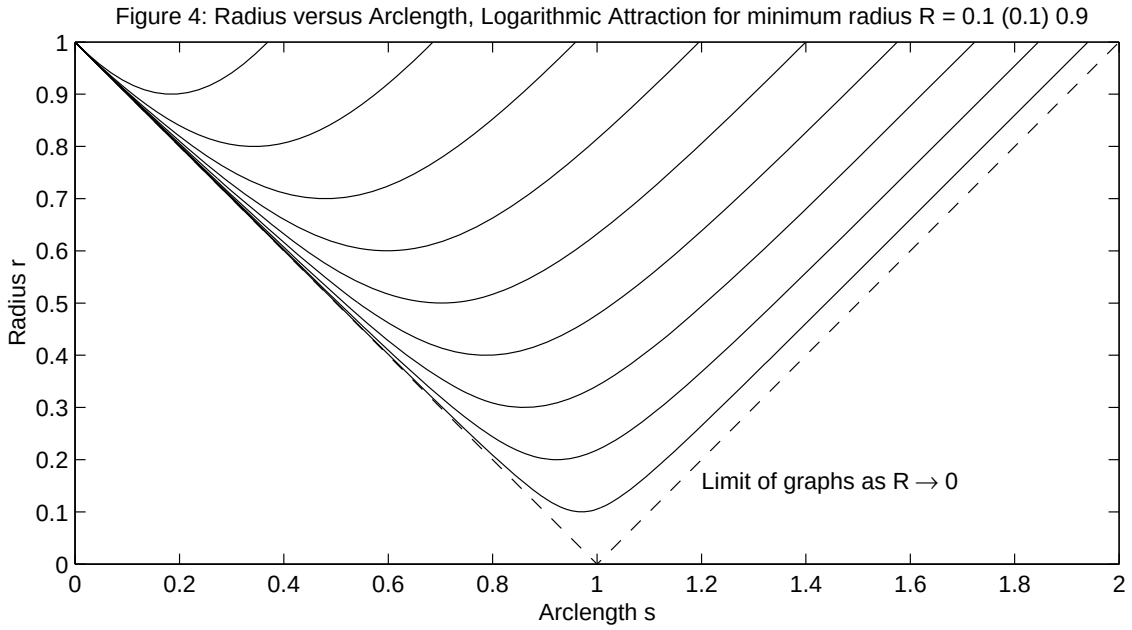

The dotted line is the limit of the graphs as $R \searrow 0$, with the first half representing the radius vector at $\vartheta = 0$, and the second half representing the radius vector at $\vartheta = \pi$.

3.3 Time as a Function of Radius

The integral (18) for t has an integrable singularity in the integrand at $\psi = 0$, and when $r = R$ it has an integrable singularity at $\psi = \log R$. Those singularities may be eliminated by an appropriate change of variable, to produce a smooth integrand which is suitable for quadrature by Romberg integration.

With the substitution (23), the equation (18) becomes

$$T(r, R) \;=\; \int_0^{\kappa(r)} \frac{\mathrm{d}\kappa}{R^{\cos\,\kappa}\,\sqrt{2\left(\mathcal{F}(\,-\log\,R\,\cos^2(\kappa/2)) - \frac{1}{\log\,R}\right)}}\;, \tag{49}$$

where the function $\kappa = \kappa(r)$ is given by (23). In particular, the time at the apse is

$$T(R, R) \;=\; \int_0^{\pi} \frac{\mathrm{d}\kappa}{R^{\cos\,\kappa}\,\sqrt{2\left(\mathcal{F}(\,-\log\,R\,\cos^2(\kappa/2)) - \frac{1}{\log\,R}\right)}}\;. \tag{50}$$

And these transformed integrals are suitable for Romberg integration with respect to κ.

3.3.1 Graphs of Radius versus Time

Figure 5 shews graphs of r versus t, for various values of the minimum radius R. Each graph is symmetric about the line $t = T(R, R)$.

Figure 5: Radius versus Time, for minimum radius R = 0.1 (0.1) 0.9

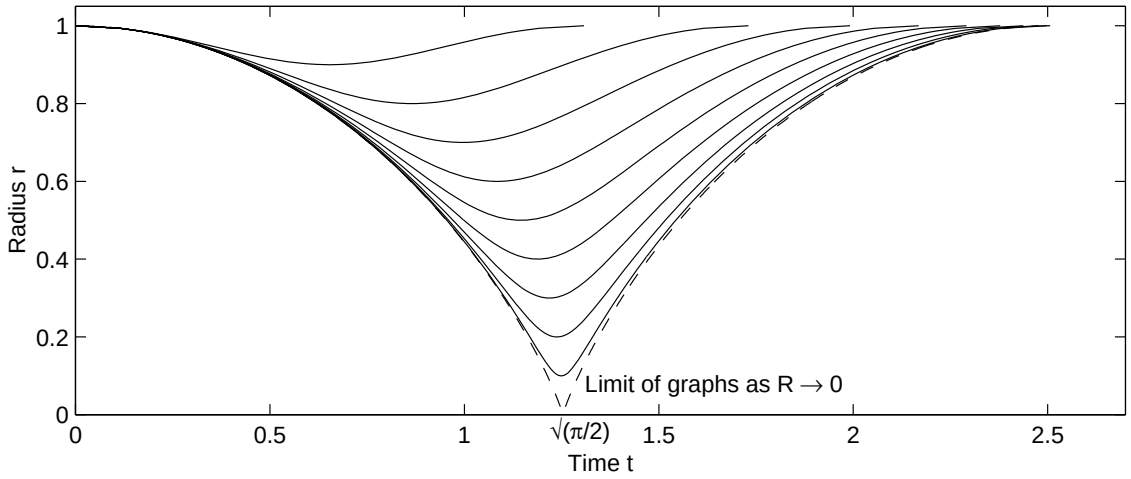

The dashed curve is the limit of the graphs as $R \searrow 0$, with the first half (cf. Figure 1) representing free fall down the radius vector at $\vartheta = 0$, and the second half representing free rise up the radius vector at $\vartheta = \pi$.

3.4 Relation between Arclength and Angle

For each value of the minimum radius R, each of ϑ, s and t can be computed from (16), (17) (18) and (19) as functions of r.

Figure 6 shews graphs of ϑ versus s for various values of R, with the points on each graph computed for the parameter r.

Figure 6: Arclength vs. Angle, Attractive Logarithmic Potential for minimum radius R = 0.1 (0.1) 0.9

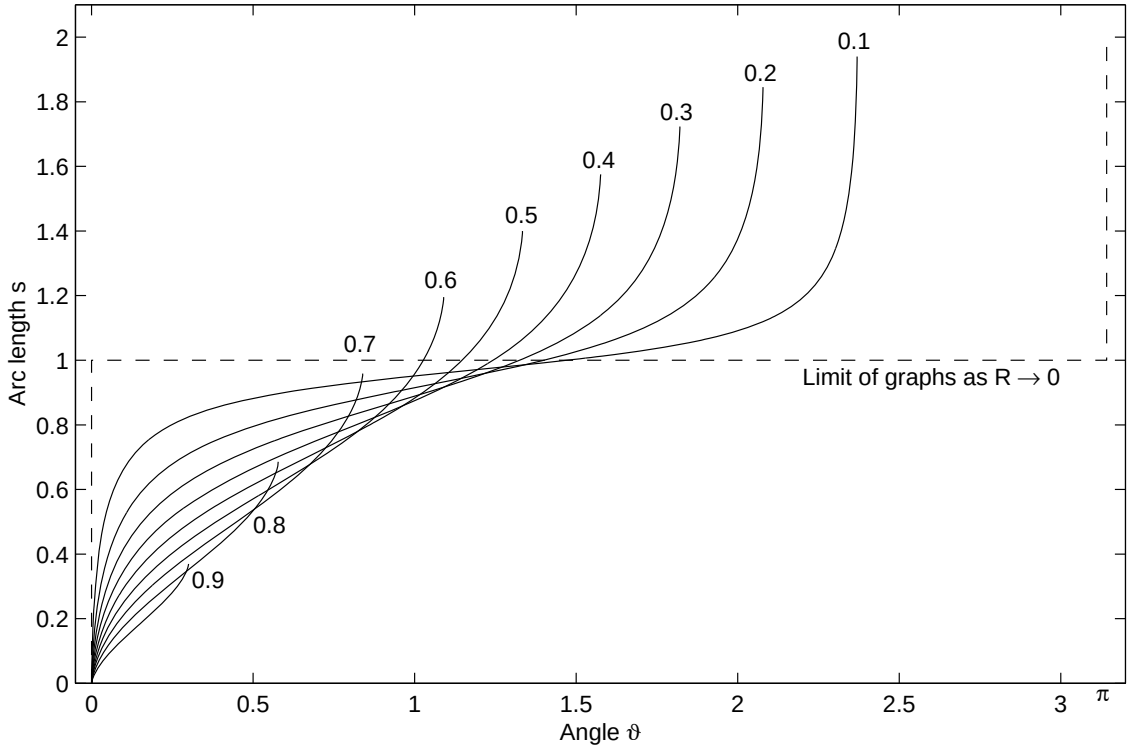

The dashed line is the limit of the graphs as $R \searrow 0$, with the first vertical line representing the radius vector at $\vartheta = 0$, and the second vertical line representing the radius vector at $\vartheta = \pi$. The horizontal line represents the transition from the first radius vector to the second, with zero arclength involved.

Since angle (20) arclength (21) (and likewise time (22)), measured from the apse, are each even functions of r, each of these graphs is symmetric about its midpoint, corresponding to the apse.

3.5 Relation between Time and Angle

Figure 7 shews graphs of t versus ϑ for various values of R, with the points on each graph computed for many values of the parameter r. Since both angle (20) and time (22) , measured from the apse, are even functions of r, each of these graphs is symmetric about its midpoint, corresponding to the apse.

Figure 7: Time vs. Angle, Attractive Logarithmic Potential for minimum radius R = 0.1 (0.1) 0.9

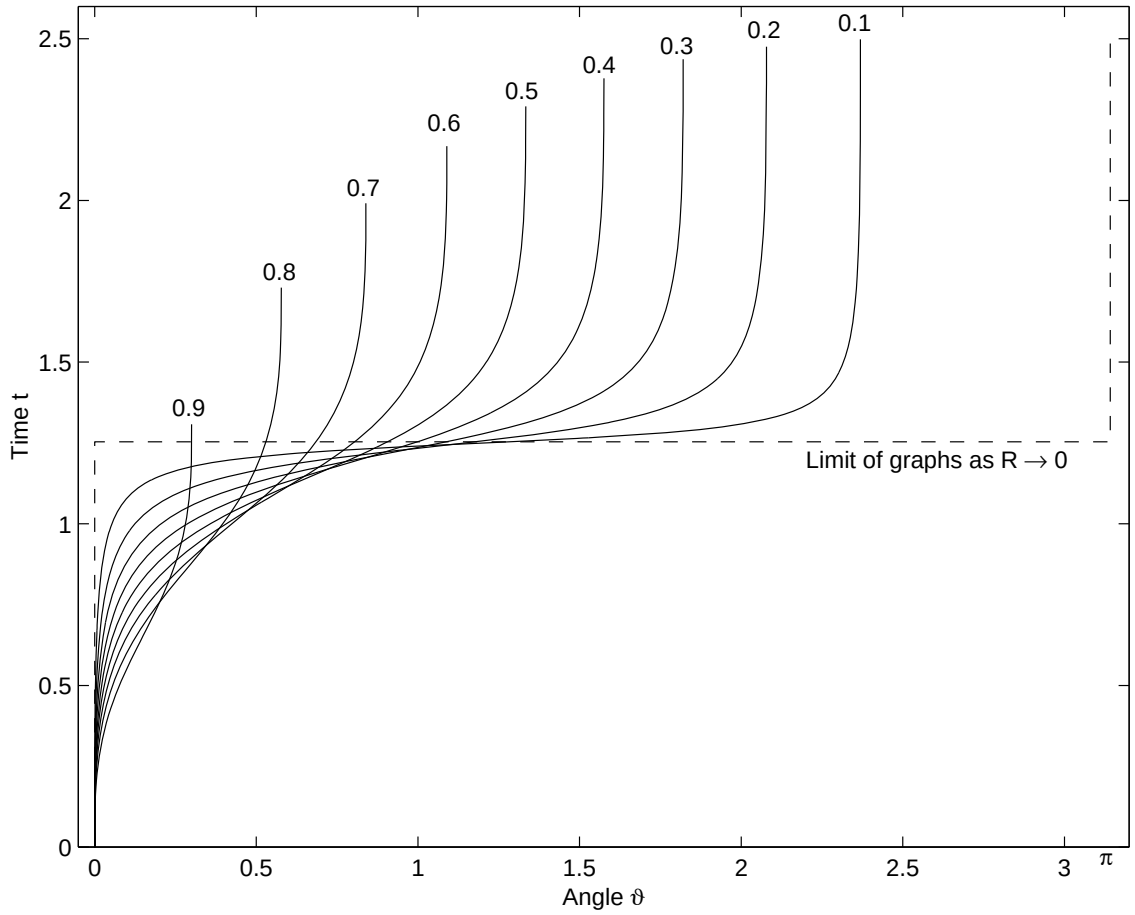

The dashed line is the limit of the graphs as $R \searrow 0$, with the first vertical line representing the radius vector at $\vartheta = 0$, and the second vertical line representing the radius vector at $\vartheta = \pi$. The horizontal line represents the transition from the first radius vector to the second, with zero time involved.

3.6 Relation between Arclength and Time

Figure 8 shews graphs of s versus t for various values of R, with the points on each graph computed for many values of the parameter r.

Figure 8: Arclength vs. Time, Attractive Logarithmic Potential for minimum radius R = 0.1 (0.1) 0.9

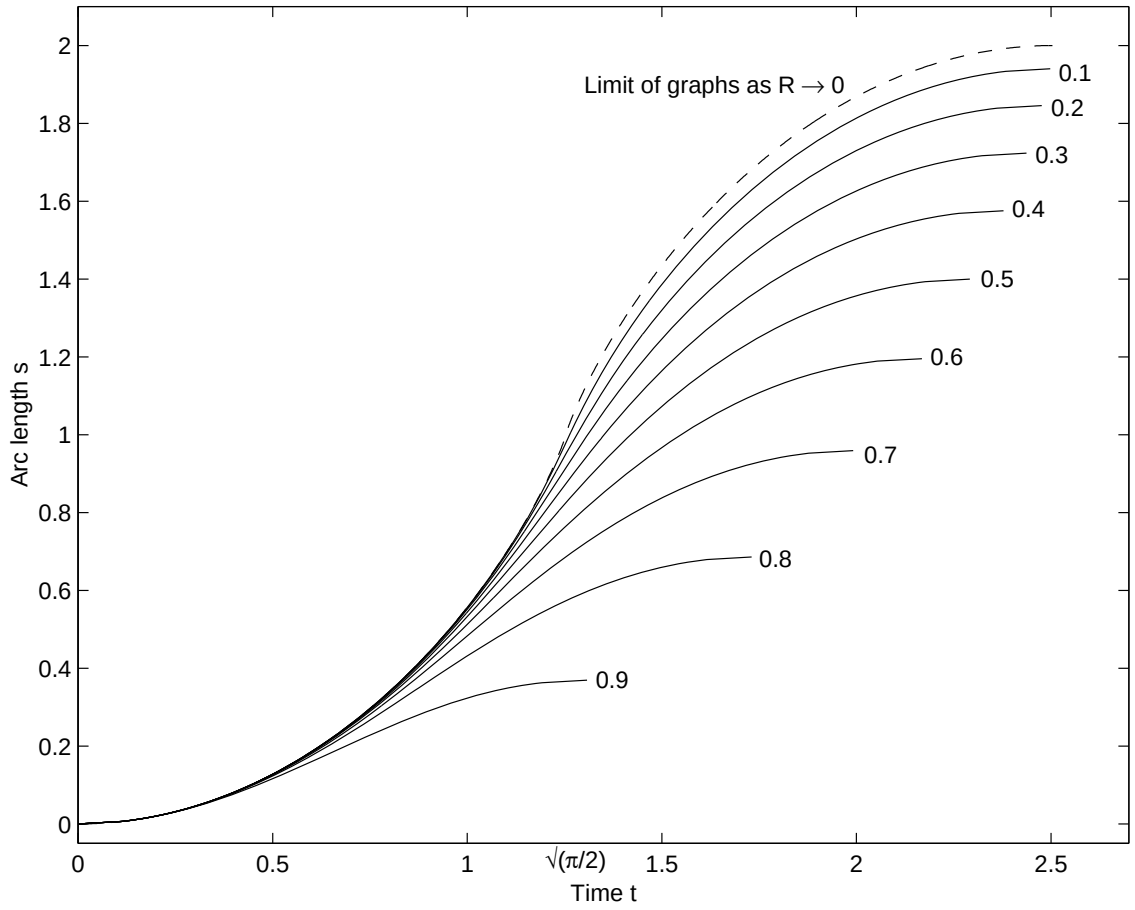

The dashed curve is the limit of the graphs as $R \searrow 0$, with the first half (cf. Figure 1) representing free fall down the radius vector at $\vartheta = 0$, and the second half representing free rise up the radius vector at $\vartheta = \pi$.

Since both arclength (21) and time (22) , measured from the apse, are even functions of r, each of these graphs is symmetric about its midpoint, corresponding to the apse.

4 Brachistochrone Through Two Points

Reasoning similar to that for inverse square attraction (Tee, 1999, §5) shews that, through each point $B = (\rho, \psi)$ (with $\rho \leq 1$ and $0 \leq \psi < \pi$), there passes 1 and only 1 brachistochrone starting at A.

In order to construct the brachistochrone AB, we need to compute its minimum radius $\tilde{R}$, which is the parameter for that particular brachistochrone starting from A and passing though B.

Note that $0 < \tilde{R} \leq \rho \leq 1$.

4.1 Computation of the Parameter $\tilde{R}$

If $0 < \psi \leq \Theta(\rho, \rho) < \frac{1}{2}\pi$, then B is on the first half-arch of the brachistochrone. Accordingly (cf. (30)), the angle at B satisfies the equation

$$\psi \;=\; \Theta(\rho, \tilde{R}), \tag{51}$$

for some minimum radius $\tilde{R} \leq \rho$.

Otherwise, B is on the second half-arch, and the angle at B satisfies the equation (19)

$$\psi \;=\; 2\Theta(\tilde{R}, \tilde{R}) - \Theta(\rho, \tilde{R}). \tag{52}$$

In particular, this is the case if $\frac{1}{2}\pi \leq \psi < \pi$.

Thus, the construction of the brachistochrone AB has been reduced to computation of the root $R = \tilde{R}$ of the equation

$$\Upsilon(R) \;=\; \psi. \tag{53}$$

For $\Theta(R, R) \geq \psi$,

$$\Upsilon(R) \;\stackrel{\text{def}}{=}\; \int_0^{\kappa(\log\,\rho)} \frac{-\log\,R\,\sin^2(\kappa/2)}{\sqrt{1 - \log\,R\,\mathcal{F}(-\log\,R\,\cos^2(\kappa/2))}}\,\mathrm{d}\kappa, \tag{54}$$

but otherwise

$$\Upsilon(R) \;\stackrel{\text{def}}{=}\; 2\Theta(R, R) - \int_0^{\kappa(\log\,\rho)} \frac{-\log\,R\,\sin^2(\kappa/2)}{\sqrt{1 - \log\,R\,\mathcal{F}(-\log\,R\,\cos^2(\kappa/2))}}\,\mathrm{d}\kappa\;. \tag{55}$$

Here, $\kappa(\psi)$ is defined by (24), and $\mathcal{F}(w)$ is defined by (31).

The equation (53) can readily be solved to high accuracy by the secant method, which requires evaluation of the function Υ and which requires two initial estimates of the root — e.g. $R_0 = 0{\cdot}9\rho,\ R_1 = 0{\cdot}7\rho$. When the pair of initial estimates are such that the secant method does converge to a root ($R_n \to \tilde{R}$), then it converges (for a C^2 function) with order $\gamma = (\sqrt{5}+1)/2 = 1{\cdot}6180340$. Since the convergence is of order $\gamma > 1$ (which is faster than linear), then $(R_n - \tilde{R})/(R_n - R_{n-1}) \to 0$ as $n \to \infty$, and so the limit $\tilde{R}$ can reliably be estimated.

Once $\tilde{R}$ has been computed, then the arclength AB can be computed from (47), and the minimum passage time from A to B can be computed from (49).

4.2 Examples of Construction of Brachistochrone Through Two Points

Many examples of brachistochrones through two points have been computed by a program written in Lightspeed PASCAL, using extended variables which have round-off corresponding to 18 or 19 significant decimal figures. Some examples are presented in Table 2, with initial estimates based on Figure 3. In each case, the secant method ended with two successive estimates of R differing by less than 10^{-16}. (Some other initial estimates R_0 & R_1 gave divergence.)

Here, ρ and ψ give the polar coordinates of the endpoint B,
R_0 and R_1 are the initial estimates given for apse radius R,
Steps is the number of steps performed of the secant method,
$\tilde{R}$ is the computed value for R,
s is the arclength of the brachistochrone AB, and
t is the time for the particle to reach the endpoint B.

Table 2

ρ	ψ	R_0	R_1	**Steps**	**Brachistochrone** AB
1·0	0·157	0·996	0·99	6	$\tilde{R} = 0{\cdot}948788343797909$ $s = 0{\cdot}196476503746508$ $t = 0{\cdot}968394666245991$
0·9	1·5	0·8	0·7	6	$\tilde{R} = 0{\cdot}426480927074592$ $s = 1{\cdot}430723925548911$ $t = 2{\cdot}082739096676244$
0·9	2·5	0·1	0·08	6	$\tilde{R} = 0{\cdot}062333726353732$ $s = 1{\cdot}867880510968911$ $t = 2{\cdot}059530248212051$
0·6	0·5	0·599	0·598	7	$\tilde{R} = 0{\cdot}598723464905918$ $s = 0{\cdot}571271064389208$ $t = 1{\cdot}057464760484534$
0·45	0·6	0·44	0·43	8	$\tilde{R} = 0{\cdot}443339148395256$ $s = 0{\cdot}690499643593194$ $t = 1{\cdot}124262547909142$
0·4	0·5	0·3	0·35	8	$\tilde{R} = 0{\cdot}367769532583414$ $s = 0{\cdot}683831939327019$ $t = 0{\cdot}795163104970152$
0·2	0·26	0·15	0·14	7	$\tilde{R} = 0{\cdot}098335703204582$ $s = 0{\cdot}808955636324865$ $t = 1{\cdot}168122386544447$

5 Brachistochrones For Repulsive Logarithmic Potential

The brachistochrones for repulsive logarithmic potential display some interesting complexities, associated with the radius $\sqrt{e}$.

Acknowledgments

I wish to thank Ron Keam, for stimulating discussions about this problem.

References

1. Tee, G. J. (1999), Isochrones and brachistochrones, *Dynamic Systems and Applications*, (*to appear*).
2. Tee, G. J., Brachistochrones for repulsive inverse square force, (*to appear*).

1999–1–30